

Spectra of the non-thermal radio radiation from the galactic polar regions

H. V. Cane[★] *Department of Physics, University of Tasmania, GPO Box 252C, Hobart, Tasmania, Australia 7001, and Dominion Radio Astrophysical Observatory, National Research Council of Canada, Herzberg Institute of Astrophysics, Box 248, Penticton, BC V2A 6K3, Canada*

Received 1979 May 2; in original form 1978 December 21

Summary. Measurements of the galactic radio background radiation have been made at 5.2, 9.0, 15.6 and 23.0 MHz using half-wave dipoles directed towards declinations $\delta = +49^\circ$ and $\delta = -43^\circ$. The same receiving equipment and calibration standard was used for both sets of measurements, and the temperatures of the regions closest to the galactic poles for these declinations were found to agree within 10 per cent. The data are compatible with the recent *RAE-2* satellite spectra and the southern measurements of the Sydney group. A straight spectrum from 6 to 100 MHz gives a total background spectral index of 0.55 ± 0.03 .

The observed polar spectra can be explained by a simple model consisting of a disk of uniform emission and absorption, and an extragalactic component which is responsible for about 18 per cent of the total emission at 10 MHz.

1 Introduction

Information in a number of fields of astrophysics has been sought by combining galactic non-thermal radio background spectra with other data (e.g. Webber 1968; Goldstein, Ramaty & Fisk 1970; Daniel & Stephens 1970). In particular, the polar spectra have been used by radio astronomers to assign absolute temperature levels to continuum maps at low frequencies, because of the difficulty of calibrating large arrays; the polar spectra therefore need to be well defined so that northern and southern sky surveys can be intercompared. There are, however, several problems associated with the existing data.

First, there are only a few measurements of the south polar spectrum, principally those of Yates & Wielebinski (1966) and Ellis (1965), which are inconsistent.

Secondly, comparisons of the north and south galactic polar spectra indicate a difference

[★] Present address: Department of Geophysics and Astronomy, University of British Columbia, Vancouver, Canada V6T 1W5.

in spectral index* first pointed out by Hamilton (1969) and Hamilton & Francey (1969). One suspects that this difference may be caused by the use of different instruments and techniques in the two hemispheres.

Thirdly, there is a discontinuity between the northern ground-based data and the satellite data which provide most of the information below 10 MHz.

Finally, it is difficult to combine the measurements of different workers since the data are often presented in graphical form only.

The experiment described below was designed to clarify this situation and to eliminate most of the uncertainties in comparing northern and southern data. In addition a table of all previous measurements is presented.

2 Instrumentation

2.1 AERIAL SYSTEMS

The observations were made with aerial systems which were replicas scaled in proportion to the wavelength used. At each wavelength the aerial was a single dipole, 0.5λ in length, oriented east–west at a height of 0.125λ above a $\lambda \times \lambda$ screen of parallel aluminium wires, 0.03λ apart and about 1 m above the ground. The dipole impedances were measured with an admittance bridge connected to the dipole by a 300-ohm twin lead. Lattice networks mounted at the dipole transformed the impedances to 75 ohm and acted as baluns. The lattice networks were connected to the receiver by 75-ohm coaxial cable.

The southern observations were performed at Llanherne, Tasmania, and subsequently the dipoles, matching units and coaxial cable were transported to Penticton, British Columbia, Canada.

2.2 RECEIVING EQUIPMENT

The same receiving equipment was used in each hemisphere with only minor alterations. The superheterodyne receivers were tunable from 2 to 24 MHz with a bandwidth of 2 kHz, and were adjusted to an input impedance of 75 ohm at the frequency of operation.

2.3 CALIBRATION STANDARD

The primary noise standard at all frequencies was a temperature-limited diode noise generator manufactured by Aerospace Research Inc. This had a 50-ohm load resistor and was capable of producing a maximum temperature of 1.2×10^5 K. A secondary standard used in both hemispheres consisted of a temperature-limited diode noise source (with a 75-ohm load) in series with a broadband pre-amplifier of approximately 20 dB gain and a variable attenuator. This noise source was calibrated against the primary source through a 20 dB attenuator. The maximum temperature obtainable from this secondary source was roughly 10^6 K. Since 10^6 K is less than the aerial temperature at 5 MHz, calibration at this frequency was made against the aerial signal attenuated by 6 dB.

To determine variations of aerial temperature throughout the day, solid-state noise sources were substituted for each of the aerials at the receiver end of the coaxial cable for 2 min each sidereal hour. These very stable noise sources followed a design developed by Bird, Morton & Williams (1974). The current through the transistors was adjusted so that the

* In this paper the variation of brightness I with frequency ν is expressed as $I \propto \nu^{-\alpha}$, where α is the spectral index. The temperature spectral index $\beta = 2 + \alpha$.

noise output was almost equal to the expected aerial temperature during transit of the polar region.

3 Measurement technique

3.1 SOUTHERN OBSERVATIONS

The southern observations were conducted from 1977 July to October. Interference was a serious problem, particularly at 5.2 MHz where the background could be measured only on a few nights, but at the higher frequencies about 10 good records were obtained at each frequency. The necessity of shifting the observing frequency to locate free bands introduced some uncertainties in the impedances of the aerials, although measurements of the impedances over appropriate frequency ranges after the northern experiment indicated that these systematic errors would be typically a few per cent and hence would be negligible in comparison with the random errors arising from interference and ionospheric effects, which were typically 15 per cent.

The calibration procedure consisted of replacing the aerial and feed cable by the secondary diode noise source once during each transit of the polar region ($RA \approx 00^h 40^m$), and determining the diode noise current required to produce the same deflection as the aerial.

3.2 NORTHERN OBSERVATIONS

The northern observations were carried out in 1978 from January to March. The conditions were very good and there was no need to alter frequencies during the course of the observations. The impedances of the aerials and receiver inputs were monitored and found to remain sensibly constant.

The design of the solid-state noise sources was improved prior to commencement of the northern observations, and they were found to be extremely stable. They were calibrated against the secondary diode standard, and sky temperatures were obtained by noting the levels of the sky relative to the hourly calibrations. Thus it was not necessary to substitute the secondary diode standard during transit of the polar region.

4 Results

4.1 CORRECTION FOR LOSSES

(a) *Ionosphere*

Observations were made between midnight and dawn during winter months near the minimum of the solar cycle when ionospheric absorption is minimal. f_oF_2 values during the observations were typically 1 MHz. The estimated absorption at 5 MHz for such f_oF_2 values is less than 0.1 dB (Ellis 1965), and no allowance for this effect has been made.

(b) *Ground absorption*

Tests on similar parallel-wire reflecting screens have shown that the losses should be less than 0.1 dB (Andrew 1966). Yates & Wielebinski (1966) were unable to detect any changes in aerial temperature resulting from the use of larger screens or screens laid directly on the ground.

(c) *Losses in aerial systems*

Losses in the lattice networks were expected to be less than 0.02 dB.

4.2 ACCURACY

The accuracy of absolute temperature measurements is limited by that to which the losses can be estimated, that of the noise calibrations, and by the scatter in the observations caused by ionospheric effects and low-level interference. For low-frequency measurements the last source of error can dominate the others, as is the case for the southern measurements presented here. For these measurements an accuracy of ± 15 per cent has been assigned to the three higher frequency measurements based on maximum excursions from the mean value. The 5.2-MHz estimate is based on a single observation and an error of ± 25 per cent has been assigned to this southern measurement.

The night-to-night consistency of the northern observations was better than 5 per cent for the three higher frequency measurements and better than 12 per cent for the 5.2-MHz measurement. The accuracies of (a) the primary noise source and of the inter-calibrations of the secondary sources, and (b) the measurements of cable losses and estimates of mismatch losses, are taken to be ± 3 and ± 2 per cent respectively. These values lead to a total estimated maximum error of ± 7 per cent for the higher frequency northern measurements and ± 13 per cent for the 5.2-MHz northern measurement.

4.3 RESULTS

In Fig. 1 we show the two sets of data. The measurements from each hemisphere are displaced slightly in opposite directions from the nominal frequency to facilitate comparison. The straight line through the data has a slope of 2.55 and represents the best fit

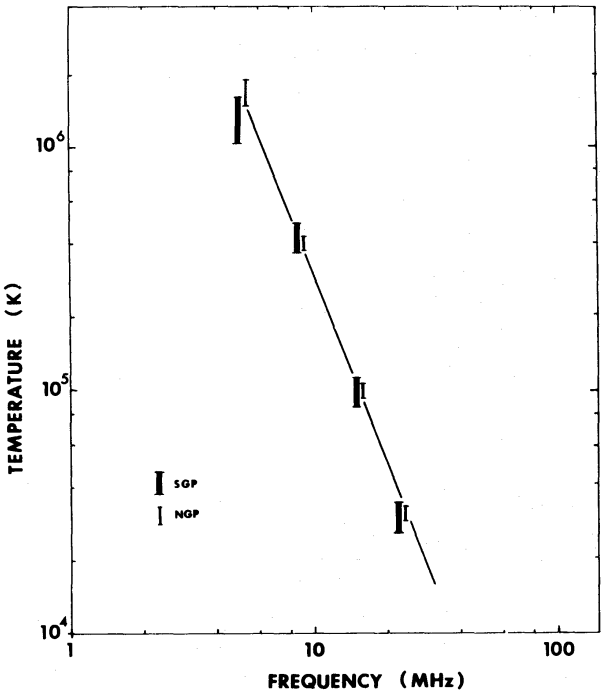


Figure 1. Measured brightness temperatures of the north and south galactic polar regions. The straight line is the best fit to representative data as discussed in the text.

Table 1. Summary of results.

Frequency (MHz)	South		North	
	Brightness temperature (K)	Brightness (W m ⁻² Hz ⁻¹ sr ⁻¹)	Brightness temperature (K)	Brightness (W m ⁻² Hz ⁻¹ sr ⁻¹)
23.0	3.0×10^4	4.9×10^{-21}	3.1×10^4	5.0×10^{-21}
15.6	9.8×10^4	7.3×10^{-21}	9.9×10^4	7.4×10^{-21}
9.0	4.2×10^5	1.0×10^{-20}	4.0×10^5	9.9×10^{-21}
5.2	1.3×10^6	1.1×10^{-20}	1.7×10^6	1.4×10^{-20}

to the existing data discussed in Section 5. Fig. 1 may thus be used for estimating average background temperatures in the frequency range 6–30 MHz. Table 1 lists the brightness temperatures and brightness values derived for the southern and northern polar regions.

5 Results of other workers and comparison with present results

Low-frequency, low-resolution spectra of the non-thermal background have been measured by many workers using a variety of techniques. Tables 2, 3 and 4 present the data and the observers for the separate polar regions. Summaries of each experiment may be found in Hamilton (1969) and Cane (1977).

In Figs 2 and 3 the filled symbols show the previous measurements of the south and north polar regions while the unfilled circles show the present results. The discontinuity near 10 MHz in the northern spectrum between ground-based and satellite data is apparent. The new data agree with the previous southern spectrum and bridge the gap between satellite and ground-based data in the north.

It should be noted that we are comparing measurements made on different parts of the sky with different beams, but these effects would not be responsible for the apparent differences between the southern and northern spectra which are resolved by the present experiment. The results of scaled antenna measurements made with steerable systems (Turtle *et al.* 1962; Bridle 1967) indicate that temperatures near the pole, for declinations between +40° and +69°, vary by approximately 10–20 per cent. Certain regions of the sky have been observed with dipoles and small arrays (Yates 1967) and the variation in high-latitude temperatures is less than 30 per cent.

We conclude that it is justifiable to inter-compare these low-resolution measurements, although in the tables and figures we have differentiated between the space-borne (S), dipole (D) and higher resolution (A) measurements. For the ground-based measurements the declination of the observations is given. Some ground-based measurements have been adjusted to the pole and for these the declination is given as NGP or SGP.

In summary, a consistent set of data has been obtained which show that the north and south polar temperatures differ by less than 10 per cent. A single spectrum is thus representative of the non-thermal background radiation at high latitudes and this can be defined by the *RAE-2* spectra, the present northern spectrum and the data of Yates & Wielebinski (1966). A straight spectrum fitted to these data above 6 MHz gives a total background spectral index of 0.55 ± 0.03 . This value is in agreement with the values of 0.55 ± 0.04 obtained by Bridle (1967) and 0.60 ± 0.05 obtained by Yates (1967).

Table 2. Spectral measurements of north galactic polar region.

Frequency (MHz)	Equivalent aerial temperature (K)	Sky brightness (W m ⁻² Hz ⁻¹ sr ⁻¹)	Type	Declination	Observer
0.25	7.3 × 10 ⁶	1.4 × 10 ⁻²²	S		15
0.29	1.1 × 10 ⁷	2.9 × 10 ⁻²²	S		15
0.36	1.5 × 10 ⁷	5.8 × 10 ⁻²²	S		15
0.43	1.6 × 10 ⁷	9.0 × 10 ⁻²²	S		15
0.45	1.6 × 10 ⁷	9.9 × 10 ⁻²²	S		15
0.45	4.0 × 10 ⁷	2.5 × 10 ⁻²¹	S		3
0.47	1.5 × 10 ⁷	9.9 × 10 ⁻²²	S		15
0.55	3.8 × 10 ⁷	3.5 × 10 ⁻²¹	S		3
0.6	1.6 × 10 ⁷	1.8 × 10 ⁻²¹	S		15
0.69	1.7 × 10 ⁷	2.5 × 10 ⁻²¹	S		15
0.7	3.5 × 10 ⁷	5.2 × 10 ⁻²¹	S		3
0.72	3.3 × 10 ⁷	5.2 × 10 ⁻²¹	S		5
0.73	1.8 × 10 ⁷	2.9 × 10 ⁻²¹	S		15
0.85	2.7 × 10 ⁷	6 × 10 ⁻²¹	S		3
0.87	1.8 × 10 ⁷	4.1 × 10 ⁻²¹	S		15
0.88	1.7 × 10 ⁷	4.1 × 10 ⁻²¹	S		15
1.0	2.3 × 10 ⁷	7 × 10 ⁻²¹	S		3
1.05	1.6 × 10 ⁷	5.5 × 10 ⁻²¹	S		15
1.1	2.2 × 10 ⁷	8.0 × 10 ⁻²¹	S		5
1.25	1.5 × 10 ⁷	7.4 × 10 ⁻²¹	S		15
1.25	2.3 × 10 ⁷	1.1 × 10 ⁻²⁰	S		10
1.3	1.5 × 10 ⁷	7.5 × 10 ⁻²¹	S		15
1.3	1.5 × 10 ⁷	8 × 10 ⁻²¹	S		3
1.45	1.5 × 10 ⁷	9.5 × 10 ⁻²¹	S		15
1.5	2.2 × 10 ⁷	1.5 × 10 ⁻²⁰	S		10
1.6	1.1 × 10 ⁷	8.7 × 10 ⁻²¹	S		5
1.75	1.6 × 10 ⁷	1.5 × 10 ⁻²⁰	S		10
1.8	1.3 × 10 ⁷	1.25 × 10 ⁻²⁰	S		15
1.91	2.0 × 10 ⁷	2.2 × 10 ⁻²⁰	S		2
2.0	1.1 × 10 ⁷	1.3 × 10 ⁻²⁰	S		10
2.0	6.2 × 10 ⁶	7.6 × 10 ⁻²¹	A	+65°	13
2.2	8.1 × 10 ⁶	1.2 × 10 ⁻²⁰	S		15
2.2	9.4 × 10 ⁶	1.4 × 10 ⁻²⁰	S		15
2.2	7.7 × 10 ⁶	1.15 × 10 ⁻²⁰	S		3
2.2	9.4 × 10 ⁶	1.4 × 10 ⁻²⁰	S		11
2.5	7.3 × 10 ⁶	1.4 × 10 ⁻²⁰	S		10

Table 2 — *continued*

Frequency (MHz)	Equivalent aerial temperature (K)	Sky brightness (W m ⁻² Hz ⁻¹ sr ⁻¹)	Type	Declination	Observer
2.7	5.4×10^6	1.2×10^{-20}	S		3
2.8	5.4×10^6	1.3×10^{-20}	S		15
2.85	1.1×10^7	2.7×10^{-20}	S		2
3.0	5.1×10^6	1.4×10^{-20}	S		10
3.0	2.6×10^6	7.1×10^{-21}	A	+65°	13
3.4	4.9×10^6	1.8×10^{-20}	S		10
3.6	4.3×10^6	1.7×10^{-20}	S		2
3.9	2.8×10^6	1.3×10^{-20}	S		15
4.0	3.1×10^6	1.5×10^{-20}	S		3
4.5	2.3×10^6	1.45×10^{-20}	S		3
4.7	3.2×10^6	2.2×10^{-20}	S		2
4.7	1.9×10^6	1.3×10^{-20}	S		15
5.0	1.1×10^6	8.1×10^{-21}	A	+65°	12
6.3	6.5×10^5	7.9×10^{-21}	A	+56°	9
7.5	6.7×10^5	1.15×10^{-20}	S		15
9.0	2.8×10^5	7.1×10^{-21}	A	+56°	9
9.1	4.0×10^5	1.02×10^{-20}	S		15
10.0	2.3×10^5	6.9×10^{-21}	D	+52°	4
10.0	3.5×10^5	1.08×10^{-20}	A	+41°	7
10.0	2.2×10^5	6.6×10^{-21}	A	+65°	12
13.0	1.1×10^5	5.7×10^{-21}	A	+56°	9
13.1	1.0×10^5	5.4×10^{-21}	D	+52°	4
13.15	9.0×10^4	4.8×10^{-21}	A	NGP	14
13.15	1.0×10^5	5.8×10^{-21}	A	NGP	6
17.5	5.4×10^4	5.0×10^{-21}	D	+52°	4
17.5	4.8×10^4	4.5×10^{-21}	A	NGP	14
17.5	5.8×10^4	5.4×10^{-21}	A	NGP	6
18.6	4.3×10^4	4.5×10^{-21}	A	+56°	9
20.0	4.3×10^4	5.2×10^{-21}	A	+65°	12
25.0	2.6×10^4	5.0×10^{-21}	D	NGP	8
25.0	1.9×10^4	3.7×10^{-21}	A	+56°	9
26.3	1.8×10^4	3.7×10^{-21}	A	NGP	14
26.5	2.0×10^4	4.2×10^{-21}	D	+52°	4
30.0	1.7×10^4	4.7×10^{-21}	A	+65°	12
35.0	1.1×10^4	4.1×10^{-21}	D	NGP	8
38.0	9.7×10^3	4.3×10^{-21}	A	+52°	1

Table 2 – continued

Frequency (MHz)	Equivalent aerial temperature (K)	Sky brightness (W m ⁻² Hz ⁻¹ sr ⁻¹)	Type	Declination	Observer
38.0	8.0 × 10 ³	3.5 × 10 ⁻²¹	D	+52°	4
38.0	7.8 × 10 ³	3.5 × 10 ⁻²¹	A	NGP	14
40.0	5.8 × 10 ³	2.8 × 10 ⁻²¹	A	+56°	9
50.0	5.0 × 10 ³	3.8 × 10 ⁻²¹	D	NGP	8
50.0	4.3 × 10 ³	3.3 × 10 ⁻²¹	A	+65°	12
75.0	1.8 × 10 ³	3.1 × 10 ⁻²¹	D	NGP	8
81.5	1.5 × 10 ³	3.0 × 10 ⁻²¹	A	+52°	1
81.5	1.1 × 10 ³	2.3 × 10 ⁻²¹	A	NGP	14
81.5	1.1 × 10 ³	2.3 × 10 ⁻²¹	A	NGP	6
110.0	700	2.6 × 10 ⁻²¹	D	NGP	8
175.0	266	2.5 × 10 ⁻²¹	A	+52°	1
178.0	169	1.6 × 10 ⁻²¹	A	NGP	14
404.0	17.9	9.0 × 10 ⁻²¹	A	NGP	14

Table 3. Spectral measurements of south galactic polar region.

Frequency (MHz)	Equivalent aerial temperature (K)	Sky brightness (W m ⁻² Hz ⁻¹ sr ⁻¹)	Type	Declination	Observer
0.25	7.8 × 10 ⁶	1.5 × 10 ⁻²²	S		15
0.29	1.24 × 10 ⁷	3.2 × 10 ⁻²²	S		15
0.36	1.7 × 10 ⁷	6.7 × 10 ⁻²²	S		15
0.42	1.85 × 10 ⁷	1 × 10 ⁻²¹	S		15
0.42	4.4 × 10 ⁷	2.4 × 10 ⁻²¹	S		16
0.44	2.2 × 10 ⁷	1.3 × 10 ⁻²¹	S		15
0.48	1.9 × 10 ⁷	1.35 × 10 ⁻²¹	S		15
0.55	3.8 × 10 ⁷	3.5 × 10 ⁻²¹	S		16
0.6	2.0 × 10 ⁷	2.2 × 10 ⁻²¹	S		15
0.7	1.9 × 10 ⁷	2.9 × 10 ⁻²¹	S		15
0.7	4.1 × 10 ⁷	6.2 × 10 ⁻²¹	S		16
0.7	4.7 × 10 ⁷	7.0 × 10 ⁻²¹	S		16
0.73	1.8 × 10 ⁷	3.0 × 10 ⁻²¹	S		15
0.87	1.7 × 10 ⁷	4 × 10 ⁻²¹	S		15
0.9	1.8 × 10 ⁷	4.5 × 10 ⁻²¹	S		15
0.9	2.2 × 10 ⁷	5.5 × 10 ⁻²¹	S		16
0.9	1.8 × 10 ⁷	4.5 × 10 ⁻²¹	D	-42°	21
1.0	2.4 × 10 ⁷	7.2 × 10 ⁻²¹	S		16
1.0	1.7 × 10 ⁷	5.3 × 10 ⁻²¹	S		15
1.26	1.3 × 10 ⁷	6.2 × 10 ⁻²¹	S		15

Table 3 – continued

Frequency (MHz)	Equivalent aerial temperature (K)	Sky brightness (W m ⁻² Hz ⁻¹ sr ⁻¹)	Type	Declination	Observer
1.3	1.3 × 10 ⁷	6.9 × 10 ⁻²¹	S		15
1.3	1.6 × 10 ⁷	8.2 × 10 ⁻²¹	S		16
1.43	1.1 × 10 ⁷	6.6 × 10 ⁻²¹	D	-42°	21
1.45	1.2 × 10 ⁷	7.9 × 10 ⁻²¹	S		15
1.65	1.0 × 10 ⁷	8.6 × 10 ⁻²¹	A	-42°	18
1.7	8.9 × 10 ⁶	7.9 × 10 ⁻²¹	S		16
1.85	9.0 × 10 ⁶	9.5 × 10 ⁻²¹	S		15
2.13	7.9 × 10 ⁶	1.1 × 10 ⁻²⁰	D	-42°	21
2.2	7.1 × 10 ⁶	1.05× 10 ⁻²⁰	S		15
2.2	7.4 × 10 ⁶	1.1 × 10 ⁻²⁰	S		15
2.3	8 × 10 ⁶	1.3 × 10 ⁻²⁰	S		16
2.3	8 × 10 ⁶	1.3 × 10 ⁻²⁰	A	-42°	18
2.7	5.4 × 10 ⁶	1.2 × 10 ⁻²⁰	S		16
2.8	5.4 × 10 ⁶	1.29× 10 ⁻²¹	S		15
3.8	4 × 10 ⁶	1.8 × 10 ⁻²⁰	A	-42°	17
3.9	2.7 × 10 ⁶	1.28× 10 ⁻²⁰	S		15
3.9	2.9 × 10 ⁶	1.35× 10 ⁻²⁰	S		15
4.0	3.7 × 10 ⁶	1.8 × 10 ⁻²⁰	S		16
4.4	2.9 × 10 ⁶	1.7 × 10 ⁻²⁰	D	-42°	17
4.5	2.4 × 10 ⁶	1.5 × 10 ⁻²⁰	S		16
4.7	1.8 × 10 ⁶	1.25× 10 ⁻²⁰	S		15
4.7	1.9 × 10 ⁶	1.31× 10 ⁻²⁰	S		15
4.8	3.0 × 10 ⁶	2.1 × 10 ⁻²⁰	A	-42°	18
5.65	1.8 × 10 ⁶	1.8 × 10 ⁻²⁰	A	-42°	17
6.5	8.5 × 10 ⁵	1.1 × 10 ⁻²⁰	S		15
9.15	6 × 10 ⁵	1.5 × 10 ⁻²⁰	A	-32°	20
9.2	3.9 × 10 ⁵	1.0 × 10 ⁻²⁰	S		15
9.2	3 × 10 ⁵	8.4 × 10 ⁻²¹	S		15
9.6	7.2 × 10 ⁵	2.0 × 10 ⁻²⁰	A	-42°	18
10.05	3.8 × 10 ⁵	1.2 × 10 ⁻²⁰	D	-42°	17
14.1	1.3 × 10 ⁵	7.7 × 10 ⁻²¹	D	-34°	24
18.3	7.5 × 10 ⁴	7.7 × 10 ⁻²¹	A	-32°	23
20.0	5.5 × 10 ⁴	6.7 × 10 ⁻²¹	D	-34°	24
30.0	1.7 × 10 ⁴	4.8 × 10 ⁻²¹	D	-34°	24
48.5	5.1 × 10 ³	3.7 × 10 ⁻²¹	D	-34°	24
55.0	4.0 × 10 ³	3.7 × 10 ⁻²¹	A	SGP	22
85.0	1.2 × 10 ³	2.7 × 10 ⁻²¹	D	-34°	24
153.0	240	1.7 × 10 ⁻²¹	A	SGP	19

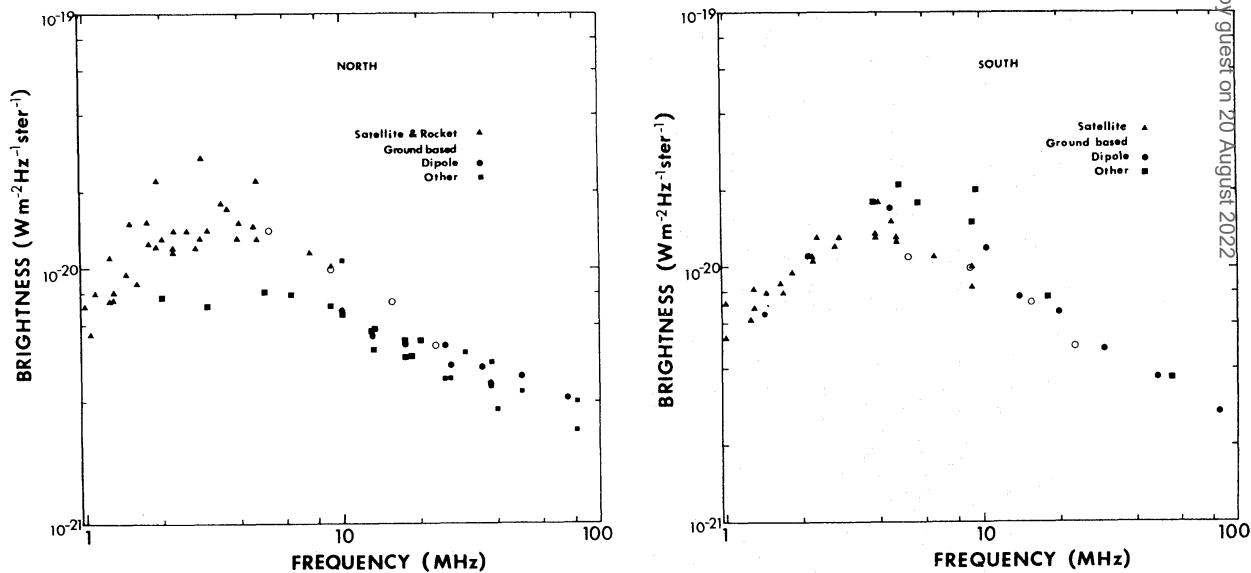
Table 4. List of observers.

1 Adgie & Smith (1956)	13 Parthasarathy (1968)
2 Alexander & Stone (1965)	14 Purton (1966)
3 Alexander <i>et al.</i> (1969a)	15 Novaco & Brown (1978)
4 Andrew (1966)	16 Alexander <i>et al.</i> (1969b)
5 Benediktov <i>et al.</i> (1965)	17 Ellis (1957)
6 Bridle (1967)	18 Ellis (1965)
7 Clark (1967)	19 Hamilton & Haynes (1969)
8 Cottony & Johler (1952)	20 Higgins & Shain (1954)
9 Getmantsev <i>et al.</i> (1969)	21 Reber & Ellis (1956)
10 Hugill & Smith (1965)	22 Rohan & Soden (1970)
11 Papagiannis (1964)	23 Shain & Higgins (1954)
12 Parthasarathy & Lorfald (1965)	24 Yates & Wielebinski (1966)

6 The 85-MHz experiment

The experimental results described above indicate that the northern and southern galactic polar regions have the same brightness temperature. The results are consistent with the southern measurements of Yates & Wielebinski (1966) but are 20–40 per cent higher than previous northern ground-based measurements, as may be seen in Fig. 2. To test the consistency of these results a further northern measurement at 85 MHz was performed.

A half-wave dipole antenna was used, 0.125λ above a ground plane of wires 0.04λ apart. The dipole was connected to 50-ohm coaxial cable by means of a Pawsey stub (Smith 1949), and the superheterodyne receiver had a reception band of 1 MHz defined at the I.F. The calibration procedure consisted of replacing the aerial at the aerial end of the feed cable by the primary diode noise source during transit of the polar region ($RA \approx 13^h 00^m$), and losses were estimated by measuring the insertion loss in an unbalanced system of two baluns back to back. The brightness temperature obtained was 1330 ± 60 K, consistent with the Yates & Wielebinski (southern) value of 1280 ± 90 K at this frequency.



Figures 2 and 3. Experimental results together with previous low-resolution measurements of the north and south galactic polar regions respectively.

7 Discussion

Fig. 4 illustrates the data, which are considered to represent the average non-thermal background spectrum at high latitudes. Spectra obtained with high-resolution instruments would deviate from this, but the spectrum can be used to investigate several astrophysical phenomena and adequately describes average properties in the solar neighbourhood.

The non-thermal radio spectrum is assumed to be produced by synchrotron radiation of cosmic ray electrons spiralling in the galactic magnetic field. The low-frequency turn-over is a result of free-free absorption of the non-thermal radiation in ionized hydrogen in the disk of the Galaxy. The simplest model that describes the high-latitude spectrum is a disk in which emission and absorption are uniformly distributed, but a better fit is obtained if an external emission component is included and this is consistent with the known contribution from extragalactic sources.

The equation describing the two-component model is

$$I(\nu) = I_g(\nu) \frac{1 - \exp[-\tau(\nu)]}{\tau(\nu)} + I_{eg}(\nu) \exp[-\tau(\nu)],$$

where $I_g(\nu)$ and $I_{eg}(\nu)$ are brightnesses at frequency ν contributed by the Galaxy and by extragalactic sources respectively, and $\tau(\nu)$ is the optical depth for the absorption.

If the emissions from the Galaxy and extragalactic sources have spectral indices of α_1 and α_2 respectively, then

$$I_g(\nu) = I_{og}\nu^{-\alpha_1} \quad \text{and} \quad I_{eg}(\nu) = I_{oeg}\nu^{-\alpha_2}.$$

α_2 is taken to be 0.8, based on observations of extragalactic sources in the frequency range 10–750 MHz (Simon 1977). Curve-fitting techniques then permit the determination of values for the four parameters I_{og} , I_{oeg} , α_1 and $\tau(\nu)$.

The properties of the Galaxy determined by the model are discussed below and in Table 5 the 10-MHz values are listed. It can be seen from Fig. 4 that the model provides a good fit to the data.

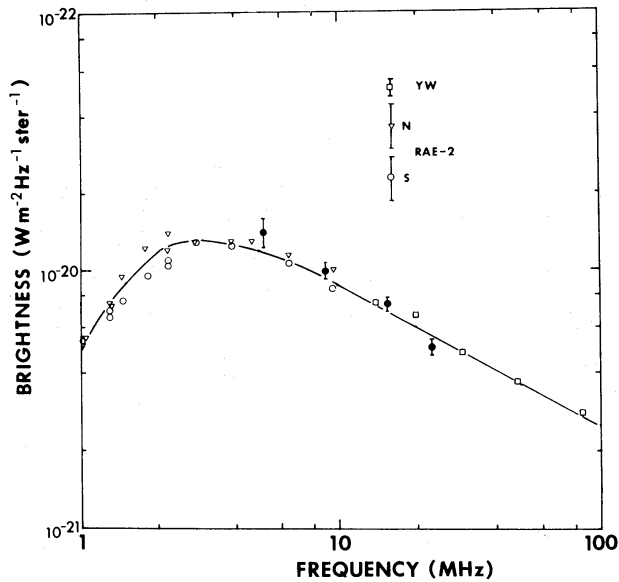


Figure 4. Present measurements (filled circles) of the galactic background together with those made by Novaco & Brown (1978) and Yates & Wielebinski (1966). The smooth curve is derived from a simple model of the Galaxy.

Table 5. Parameters of the model at 10 MHz assuming a disk of half-height 500 pc.

Synchrotron emissivity ($\text{W m}^{-3} \text{Hz}^{-1} \text{sr}^{-1}$)	Extragalactic contribution (K)	$n_e^2 T_e^{-1.35}$ ($\text{cm}^{-6} \text{K}^{-1.35}$)
$(4.9 \pm 0.3) \times 10^{-40}$	$(5.5 \pm 1.5) \times 10^4$	$(6.1 \pm 0.6) \times 10^{-8}$

(a) *The extragalactic radiation*

The extragalactic contribution at 10 MHz is determined to be $(5.5 \pm 1.5) \times 10^4 \text{ K}$. This is equivalent to a temperature of $17.5 \pm 4.5 \text{ K}$ at 178 MHz if the temperature spectral index is 2.8, which is compatible with the values obtained by Simon (1977) from source counts. Simon also calculates that the total extragalactic background should turn over between 1 and 2 MHz because of synchrotron self-absorption in the individual source components. Such an effect would not be observable if the present model is appropriate, since by 2 MHz the extragalactic radiation is almost completely absorbed in the galactic disk.

(b) *Synchrotron emissivity*

The galactic contribution to the polar brightness is found to be $(2.45 \pm 0.15) \times 10^5 \text{ K}$ at 10 MHz. This is generated over the path length L through the disk and, if this parameter is known, an estimate of the synchrotron emissivity η can be made since

$$I = \int_0^L \eta \, dl.$$

The half-height of the galactic synchrotron emission is not well determined, but the latitude distribution indicates that the emission extends to several hundred parsec perpendicular to the plane (Baldwin 1977). Using a value of 500 pc the calculated emissivity is $(4.9 \pm 0.3) \times 10^{-40} \text{ W m}^{-3} \text{Hz}^{-1} \text{sr}^{-1}$ at 10 MHz.

The synchrotron emissivity is related to the cosmic-ray electron flux in the following way:

$$\eta(\nu) \propto B_{\perp}^{(\gamma+1)/2} n_0,$$

where n_0 is the coefficient of the cosmic-ray electron spectrum which has a spectral index of γ , and B_{\perp} is the perpendicular component of the galactic magnetic field. The expected emissivity at 10 MHz, calculated from the observed electron flux (Webber 1976) assuming a magnetic field of $5 \mu\text{G}$, is $4 \times 10^{-41} \text{ W m}^{-3} \text{Hz}^{-1} \text{sr}^{-1}$ which is more than a factor of 10 below the value calculated above. Webber suggests several possible causes for the large discrepancy between the emissivities calculated from electron measurements and those from non-thermal radio spectra but the most satisfactory explanation is that the cosmic-ray electron flux observed at Earth is not typical of the flux in interstellar space.

(c) *Free-free absorption*

The optical depth for absorption in ionized hydrogen is given by

$$\tau(\nu) = 1.64 \times 10^5 T_e^{-1.35} \nu^{-2.1} E,$$

where T_e is the electron temperature in K, ν is the frequency in MHz and E is the emission measure in $\text{cm}^{-6} \text{pc}$. If $\tau(\nu) = F \nu^{-2.1}$, the fit to the data gives $F = 5 \pm 0.5$. If $F = 5$, then

$n_e^2 T_e^{-1.35} dl \approx 3.05 \times 10^{-5} \text{ cm}^{-6} \text{ K}^{-1.35} \text{ pc}$. The half-height of the emitting and absorbing disk was taken to be 500 pc, so that

$$n_e^2 T_e^{-1.35} = 6.1 \times 10^{-8} \text{ cm}^{-6} \text{ K}^{-1.35}.$$

The form of the ionized hydrogen responsible for the high-latitude absorption is not determined. If $T_e \approx 6000 \text{ K}$, then $n_e = 0.1 \text{ cm}^{-3}$. This temperature is typical of H II regions but the density is too low and it is unlikely that hydrogen ionized by young stars would extend so far from the galactic plane. Although an optical depth of 5 at 1 MHz could be realized in a small H II region close to the Sun, the shape of the low-frequency end of the background spectrum is indicative of more uniform mixing of emission and absorption. If the absorption is due to partially ionized H I with an electron density of 0.03 cm^{-3} then the electron temperature obtained is 1200 K.

(d) Spectral index of the galactic component

α_1 is determined to lie in the range of 0.50–0.53.

Finally, it appears that a two-component model can adequately describe the high-latitude background spectrum. It cannot, however, describe higher resolution observations near the galactic plane, and a more detailed model has been constructed (Cane 1977) which will be discussed in a future publication.

Acknowledgments

The work was a joint project between the University of Tasmania and the NRC of Canada. Funds for the transport of equipment, provided by the Physics Department of the University of Tasmania, are gratefully acknowledged as is the financial support of the NRC. Technical assistance was provided by P. E. N. Button and A. Vrana in the south, and G. A. Plassmann, T. L. Landecker and A. R. Hamilton in the north. The author thanks the staff of the Dominion Radio Astrophysical Observatory for their hospitality and A. Pedlar and T. L. Landecker for the useful discussions during the preparation of this manuscript.

References

- Adgie, R. & Smith, F. G. 1956. *Observatory*, **76**, 181.
- Alexander, J. K., Brown, L. W., Clark, T. A., Stone, R. G. & Weber, R. R., 1969a. *Astrophys. J.*, **157**, L163.
- Alexander, J. K., Brown, L. W., Clark, T. A., Stone, R. G. & Weber, R. R., 1969b. Presented at the American Astro. Soc. Meeting held in New York, December 8–11.
- Alexander, J. K. & Stone, R. G., 1965. *Astrophys. J.*, **142**, 1327.
- Andrew, B. H., 1966. *Mon. Not. R. astr. Soc.*, **133**, 463.
- Baldwin, J. E., 1977. In *The Structure and Content of the Galaxy and Galactic Gamma Rays*, NASA CP-002 US Government Printing Office, Washington, p. 189.
- Benediktov, E. A., Getmantsev, G. G., Mitjakov, N. A., Rapoport, V. O., Sazonov, J. A. & Tarasov, A. F., 1965. *Space Res.*, **VI**, 110.
- Bird, I. G., Morton, B. R. & Williams, H. A., 1974. *Proc. Instn Radio Engrs Aust.*, **35**, 133.
- Bridle, A. H., 1967. *Mon. Not. R. astr. Soc.*, **136**, 219.
- Cane, H. V., 1977. *PhD thesis*, University of Tasmania.
- Clark, T. A., 1967. *PhD thesis*, University of Colorado.
- Cottony, H. V. & Johler, J. R., 1952. *Proc. Inst. Radio Engrs*, **40**, 1053.
- Daniel, R. R. & Stephens, S. A., 1970. *Space Sci. Rev.*, **10**, 599.
- Ellis, G. R. A., 1957. *J. geophys. Res.*, **62**, 229.
- Ellis, G. R. A., 1965. *Mon. Not. R. astr. Soc.*, **130**, 429.

- Getmantsev, G. G., Karavanov, V. S., Korobkov, Yu. S. & Tarasov, A. F., 1969. *Soviet Astr. A.J.*, **12**, 5.
- Goldstein, M. L., Ramaty, R. & Fisk, L. A., 1970. *Phys. Rev. Lett.*, **24**, 1193.
- Hamilton, P. A., 1969. *PhD thesis*, University of Tasmania.
- Hamilton, P. A. & Francey, R. J., 1969. *Nature*, **224**, 1090.
- Hamilton, P. A. & Haynes, R. F., 1969. *Aust. J. Phys.*, **22**, 839.
- Higgins, C. S. & Shain, C. A., 1954. *Aust. J. Phys.*, **7**, 460.
- Hugill, J. & Smith, F. G., 1965. *Mon. Not. R. astr. Soc.*, **131**, 137.
- Novaco, J. C. & Brown, L. W., 1978. *Astrophys. J.*, **221**, 114.
- Papagiannis, M. D., 1964. *PhD thesis*, Harvard.
- Parthasarathy, R., 1968. *Proc. astr. Soc. Aust.*, **3**, 94.
- Parthasarathy, R. & Lerfald, G. M., 1965. *Mon. Not. R. astr. Soc.*, **129**, 395.
- Purton, C. R., 1966. *Mon. Not. R. astr. Soc.*, **133**, 463.
- Reber, G. & Ellis, G. R. A., 1956. *J. geophys. Res.*, **61**, 1.
- Rohan, P. & Soden, L. B., 1970. *Aust. J. Phys.*, **23**, 223.
- Shain, C. A. & Higgins, C. S., 1954. *Aust. J. Phys.*, **7**, 130.
- Simon, A. J. B., 1977. *Mon. Not. R. astr. Soc.*, **180**, 429.
- Smith, R. A., 1949. *Aerials for Metre and Decimetre Wave-lengths*, University Press, Cambridge.
- Turtle, A. J., Pugh, J. E., Kenderdine, S. & Pauliny-Toth, I. I. K., 1962. *Mon. Not. R. astr. Soc.*, **124**, 297.
- Webber, W. R., 1968. *Aust. J. Phys.*, **21**, 845.
- Webber, W. R., 1976. *Proc. astr. Soc. Aust.*, **3**, 1.
- Yates, K. W., 1967. *PhD thesis*, University of Sydney.
- Yates, K. W. & Wielebinski, R., 1966. *Aust. J. Phys.*, **19**, 389.